



# High-accuracy measurement system for the refractive index of air based on a simple double-beam interferometry

HONGTANG GAO,<sup>1,2,\*</sup> ZHONGYU WANG,<sup>1</sup> WEI ZOU,<sup>2</sup> YUZHANG LIU,<sup>1</sup> AND SHUANGHUA SUN<sup>2</sup>

<sup>1</sup>School of Instrumentation and Optoelectronic Engineering, Beihang University, Beijing 100191, China

<sup>2</sup>Division of Geometric Metrology, National Institute of Metrology, Beijing 100029, China

\*htgao@nim.ac.cn

**Abstract:** A measurement system based on a simple double-beam interferometry is built to realize the measurement of air refractive index with high accuracy. The basic principle of the system is that, through measuring the change of optical path difference caused by rapid and smooth vacuumization, measurement of refractive index of air is converted to length measurement. Error correction and signal processing are studied to ensure high-accuracy measurement of the refractive index of air. Three applicable methods are used in system. The system based on the methods realize the subdivision and counting of interference fringe by software with three-error correction, error compensation for the end-window plates' thickness change caused by vacuumization, steady realization of high vacuum conditions. To verify the accuracy and reliability of the system, the measurement results are compared with that obtained from the method based on empirical Edlén's formula. Analysis result shows that the expanded measurement uncertainty of the system is  $U = 5 \times 10^{-9}$ , with  $k = 2$ . The system can be used to compensate the laser wavelength error caused by the refractive index of air with high accuracy.

© 2021 Optical Society of America under the terms of the [OSA Open Access Publishing Agreement](#)

## 1. Introduction

Length measurement by laser interferometry is a necessary method for realizing high-accuracy measurement. However, length measurement by laser interferometry is generally done in air, where the effect of the refractive index of air limits the accuracy of the method. Exploring the measurement of refractive index of air and its error compensation is critical to improve length measurement accuracy in air. The necessity for high-accuracy measurement of the refractive index of air is obvious in the field of length metrology. For example, at present, the length value dissemination of metrology primary standard of most countries in the world are carried out under air conditions. The measurement accuracy of the primary standard is mainly limited by measurement and compensation accuracy of the refractive index of air. High-accuracy measurement of the air refractive index has always been one of important research content for researcher in the field of length metrology. A traditional double-beam interference method for measuring the refractive index is the Rayleigh interference. The technical features of the Rayleigh interferometry are that it generally uses a white light as light source, and it must be viewed under high magnification for its close-space fringes, a point or line source must be used to obtain fringes with good visibility [1]. The use of white light as light source limits its measurement range and the use of the glass plate as the optical-path compensator decrease its measurement accuracy for refractive index of air, generally the best measurement accuracy based on the methods is in the order of  $10^{-8}$ .

With the development of laser technology, various new measurement methods have emerged, such as F-P interferometry based on multi-beam interference [2–4] and the method based on a femtosecond laser [5–7]. Research has shown that many methods can be used to measure the

refractive index of air, however, there are a few convenient and practicable technologies with a measurement accuracy higher than  $1 \times 10^{-8}$  using a simple system [8–11]. Length measurement based on the laser interferometry would not be widely used today without the methods and technical measures of the refractive index of air to guarantee its accuracy [12], and with the need of increasing accuracy for length measurement primary standard, uncertainty less than  $1 \times 10^{-8}$  for the error compensation of the refractive index of air is necessary to be realized by a simple system. But it is not easy to obtain this technical specification by a simple measurement system. The target of the work is to overcome the difficulty by using some applicable methods. The main highlights of this paper are as follows:

- a. The methods of steady realization of high vacuum conditions for the measurement of the refractive index of air.
- b. One signal processing method is introduced to realize subdivision and counting of interference fringes with three-error correction based on software and a novel time-sharing sampling and recording technique.
- c. An applicable error compensation method is adopted. The micro-displacement error caused by deformation of the end-windows during vacuumization is measured and compensated by an interference unit.

One high-accuracy measurement system for the refractive index of air is introduced and realized by adopting the mentioned methods.

## 2. Components and working principle of the system

### 2.1. Basic principle of the system

The measurement principle of the system is to convert the value of the refractive index of air into that of the coherent length of an optical path by measuring the optical path change  $\Delta l$  caused by the refractive index of air at sampling length  $l$ . The difference between the refractive index of air and the vacuum refractive index which is 1 is deduced through Eq. (1), then the value of the refractive index of air is calculated according to Eq. (2).

$$\Delta n_{air} = n_{air} - 1 = \frac{\Delta l}{l} \quad (1)$$

$$n_{air} = 1 + \Delta n_{air} \quad (2)$$

The advantage of transformation from measurement of the refractive index of air to length is that the related technical methods and measures for ensuring the length measurement accuracy based on interferometry can be utilized.

### 2.2. Components of the system

The components and working principle of the system are displayed in Fig. 1. The system is mainly composed of two parts which are the optical part and mechanical and electronic part, the photo of the optical part is as shown in Fig. 2. The main components of the system include a quartz tube and its two end windows, a frequency-stabilized laser source, a laser beam collimator, a KOSTER prism, a signal processing system, a temperature measurement system, a vacuum system and its throttle valves and pipelines, a phase regulator, two photoelectric receivers and three reflectors. The quartz tube used for vacuumization is considered as the core part of the system, with a cavity length of 1 m and glass end windows (with a thickness of 6 mm) having appropriate flatness at each end. The laser beam is incident on the KOSTER prism through the laser beam collimator; the KOSTER prism splits the laser into two beams and transmits one of

them into the glass cavity which can be vacuumized while the other laser beam is transmitted into the air cavity which is formed by two glass end-windows. The quartz tube has a port which is connected to the vacuum molecular pump and vacuum gauge system through vacuum throttle valves. In terms of the basic working process, firstly, the system rapidly pumps out the air in the cavity of the quartz tube through the molecular pump until the air pressure reaches  $10^{-4}$  hPa, and counts the interference fringes caused by changing of optical path caused by vacuumization at the same time; secondly, change of the count is recorded in real-time and eventually value of air refractive index is obtained. To reduce the error induced by the complexity of the optical system, the optical system needs to be employed as simple as possible.

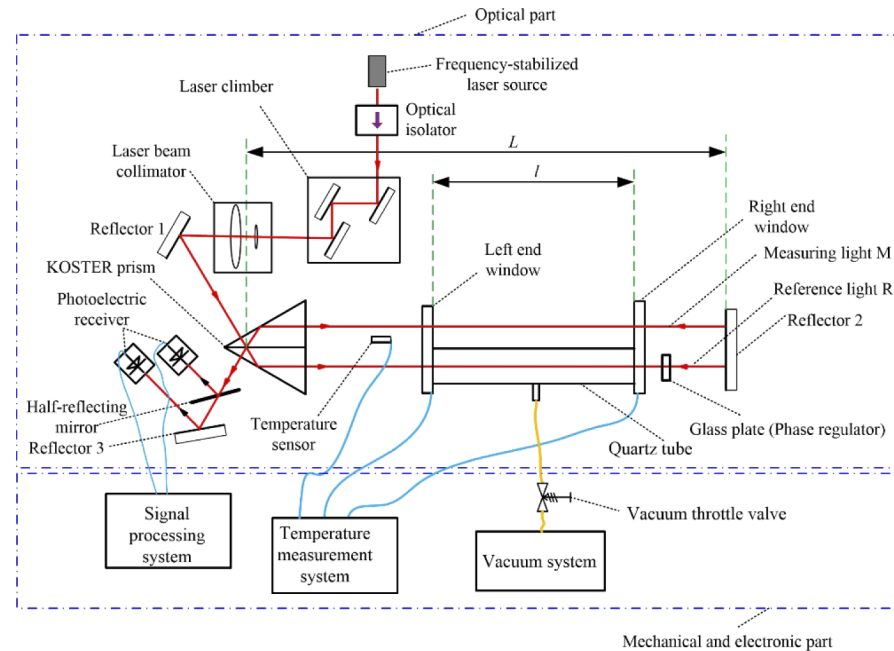


**Fig. 1.** The components and working principle of the system.

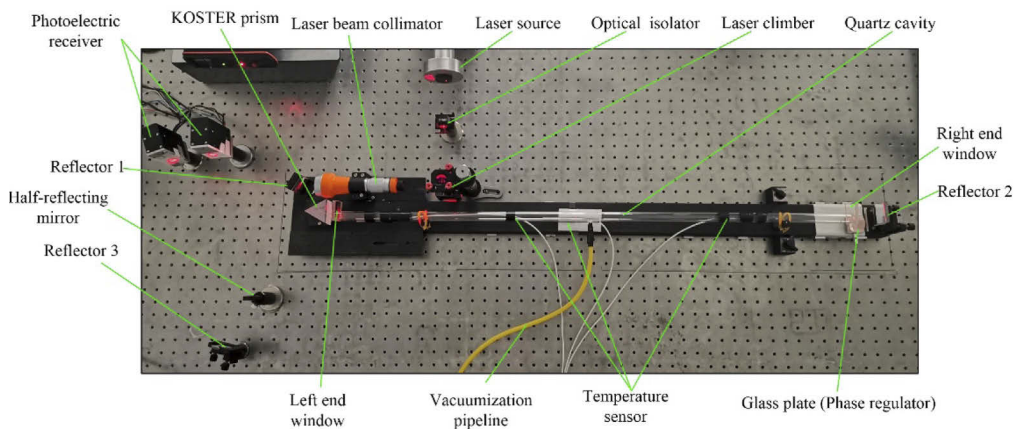


**Fig. 2.** The photograph of optical part.

### 3. Key methods used in the system

#### 3.1. Rapid and steady realization of high vacuum conditions

The reference optical path needs to be in a high vacuum cavity when measuring the refractive index of air by using two-path interferometry, with the vacuum maintained at  $1 \times 10^{-2}$  Pa [13]. It is beneficial to improving the accuracy and efficiency of the measurement of the refractive index of air with rapid and steady realization of high vacuum in the cavity. Therefore, it is necessary to minimize the duration of vacuumization. For rapid vacuumization, the vacuum pump and the sealing technology for pipelines connected thereto play a crucial role. In addition, rapid vacuumization must be done while considering the frequency and amplitude stability of the interference fringe signals to lower the subdivision and counting error of interference signals in the signal processing system. Therefore, the two-stage vacuumizing system is employed, involving vacuumization with a mechanical pump in the first stage and vacuumization with a molecular pump in the second stage. The former aims to vacuumize the vacuum pipeline system to the order of magnitude of 1 Pa in advance while the latter is expected to vacuumize and remain the vacuum cavity and pipelines connected within 0.01 Pa. The two-stage vacuumizing system can improve the vacuumizing efficiency.

Rapid vacuumization is necessary step to improve the measurement efficiency while guaranteeing the stability of vacuumization is an important step for enhancing the accuracy. How to realize steady vacuumization is analysed. Theoretically, the relationship of air pressure, flow, and flow rate in pipelines conforms to the Bernoulli equation for gas flow, as shown in Eq. (3):

$$C = \frac{p}{\gamma} + \frac{V^2}{2g} \quad (3)$$

where,  $p$  and  $V$  denote pressure intensity, and velocity of fluid particles, respectively;  $\gamma$ ,  $g$ , and  $C$  represent the bulk density of the fluid, gravitational acceleration, and a constant (the total mechanical energy of unit mass of fluid particles, that is, total head), respectively [14]. If the technical scheme on automatic control based on the theory given in Eq. (3) is applied, the gas parameters need to be sensed and adjusted by using an electric controllable valve. As a result, the complexity and cost of the system will increase. Through experiments, by employing manual throttle valves with favourable vacuum sealing performance, the interference signal is monitored manually in real time, and the throttle valve can be adjusted smoothly in real time to ensure that the signal meets design requirements. The rapid and steady vacuumization process to measuring the refractive index of air obtained by manually controlling and adjusting the flow valves is shown as Fig. 3. A group of interference signal under steady vacuumization is shown in Fig. 3(a). The vacuumization speed and the stage are shown as Fig. 3(b), when it is in a free stage of control, the vacuumization speed is in rapid linear downturn. But when it is in a stage of control, the vacuumization speed is in a linear uptrend with small fluctuation. Finally, the average speed of vacuumization is maintained at about  $2\mu\text{m/s}$ .

#### 3.2. Phase quadrature of the interference fringes

Generally, the natural change of the refractive index of air is non monotonic. In order to measure the refractive index of air with high accuracy, it is necessary to count the interference fringes reversibly when processing interference signals. The generation of interference signals with phase quadrature is the basis for reversible counting. The method includes two steps, the first step is to approximately make sure of phase quadrature of interference fringes by optics, and the second step is to accurately make sure of phase quadrature of interference signals by signal processing. This section introduces the optical method, and the method based on signal processing is introduced in the next section. There are a few ways to achieve phase quadrature of interference fringes optically. Considering the simpleness of the optical system and the signal processing system

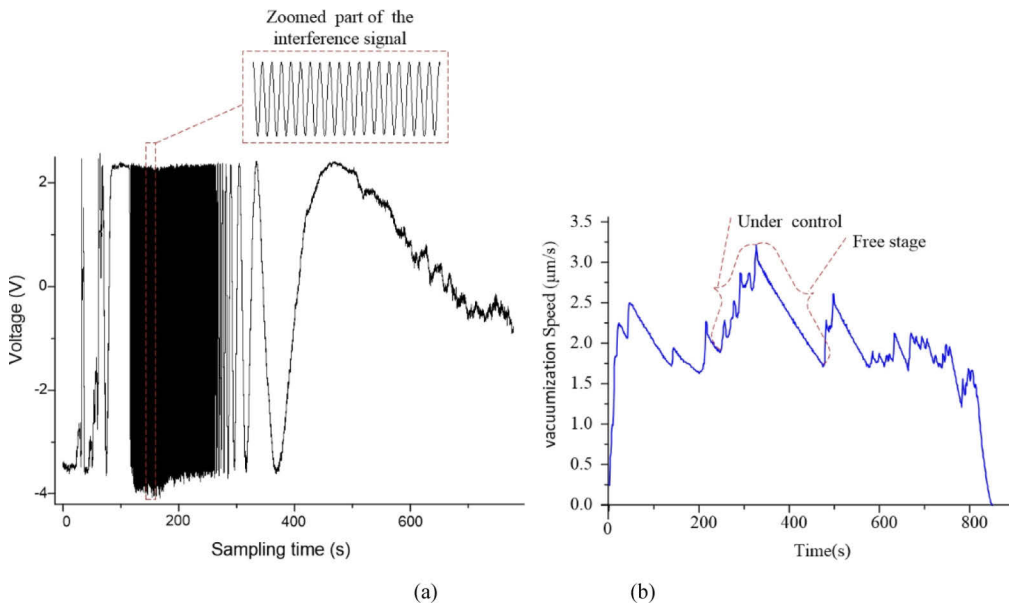


**Fig. 3.** The process of steady vacuumization: (a) interference signal under vacuumization; (b) Vacuumization speed and stage.

further make sure of the phase quadrature of the interference signals. A simple and low-cost method which well match the optics of the system is adopted. As shown in Fig. 4, a glass plate is placed at the location of optical path of the reference light, which divides the reference light beam into section A and section B. Since section A of light does not pass through the glass plate and section B of light passes through the glass plate, there is an optical path difference between two sections of light, which is caused by the glass plate. The optical path of the section A of light can be changed by rotating the glass plate. The interference occurs when the reference light and the measuring light emitting from the optical system and meeting. As shown in Fig. 5, two group of interference fringes with two sections of A and B are obtained by the half-reflecting mirror and reflector 3 in Fig. 1, which reflect the interference image to the areas A of receiver X and B of receiver Y. The phase quadrature of two group of interference fringes can be achieved by rotating the glass plate, so the glass plate is also named as phase regulator. Besides, it is necessary to properly receive and convert the interference fringe to the electric signal for the phase quadrature of the interference signal. The receiving and converting method is decided by practice, a square hole whose size is nearly the same as the width of the interference fringe( $W$ ) is placed in the front of photoelectric receiver is fitted to the system.

### 3.3. Signal processing method

The signal processing method is critical for realizing high-accuracy measurement of the refractive index of air, which includes signal filtering, three-error compensation for interference signals, and subdivision and counting of interference signals.

#### 3.3.1. Three-error compensation for interference signals

Theoretically, the interference signals of displacement are ideal sine and cosine signals with equivalent amplitude and quadrature phase and without signal bias. Due to non-ideal characteristics of the optical and circuit system, it is impossible that the interference signals show equivalent amplitude and quadrature phase and no bias. Owing to the factors are generated not by the reason

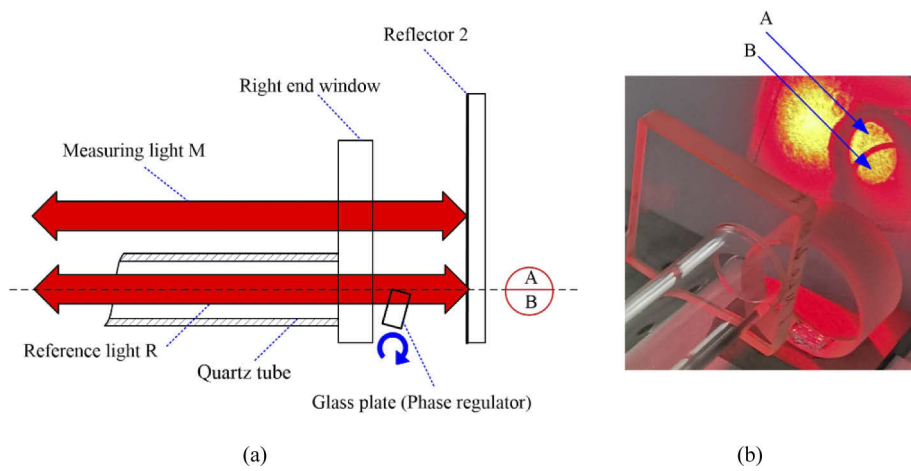


**Fig. 4.** The principle of interference signals phase adjustment: (a) Principle; (b) Photograph.

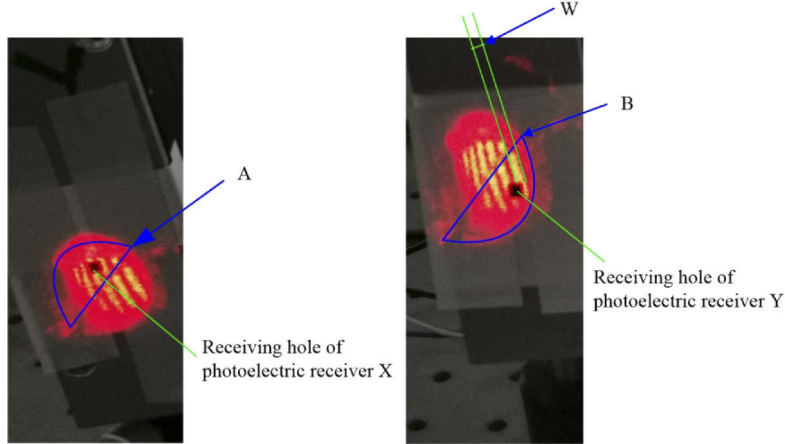


**Fig. 5.** The image of interference fringe to the receivers.

of the displacement, the error will occur if the interference signals are not processed. The three non-ideal factors existing in interference signals will lead to a displacement measurement error (the three errors of interference signals). It is necessary to analyze the displacement error caused by the three errors of interference signals to perform the correction. The interference signals with three errors can be expressed as follows:

$$\begin{cases} u_{1d} = u_1 + p \\ u_{2d} = \frac{u_2 \cos \alpha - u_1 \sin \alpha}{G} + q \end{cases} \quad (4)$$

where,  $u_{1d}$  and  $u_{2d}$  refer to interference signals;  $\alpha$  and  $G$  separately denote the non-quadrature error and the ratio of amplitudes of two-path signals;  $p$  and  $q$  separately denote for the direct current levels of interference signals  $u_{1d}$  and  $u_{2d}$ . The phase of the displacement obtained from the two-path interference signals is calculated as follows:

$$\theta = \arctan(u_{1d}/u_{2d}) \quad (5)$$

Due to the presence of three errors in the interference signals, the phase shows error  $\delta_\theta$ , which can be expressed as follows:

$$\delta_\theta = \frac{\sin \theta \cos \theta (\cos \alpha - G) - \cos^2 \theta \sin \alpha}{G} + \frac{1}{R}(q \cos \theta + p \sin \theta) \quad (6)$$

On condition of  $G \rightarrow 1$  and  $\alpha \rightarrow 0$ , errors above second order are ignored. Equation (6) is simplified as follows:

$$\delta_\theta \approx \frac{1-G}{2} \sin 2\theta - \alpha \cos^2 \theta + \frac{\sqrt{p^2 + q^2}}{R} \sin(\theta - \arctan \frac{q}{p}) \quad (7)$$

It can be seen from Eq. (7) that the  $\frac{1-G}{2}$  maximum error introduced by in-equivalent amplitudes is the maximum at  $\theta = \frac{\pi}{4}, \dots$ ; the maximum error introduced by non-quadrature error corresponds to radius  $\alpha$ , whose maximum appears at  $\theta = 0, \pi, \dots$ ; the maximum error introduced by signal bias corresponds to  $\frac{\sqrt{p^2 + q^2}}{R}$ , whose position depends on the values of  $p$  and  $q$ . Owing to the peaks of three errors not being in the same position, the comprehensive influence of the three errors is less significant than the influence of the sum of their own maximum. If the calculation results are corrected according to Eq. (6) by directly applying simple error compensation, it is applicable to the condition of low values of each of the three errors due to non-linear factors influencing error compensation. To attain a correction method with strong applicability for the three errors, the interference signals with the three errors are further analyzed. The actual interference signals are described by using an elliptic equation:

$$(u_{1d} - p)^2 + \left[ \frac{(u_{2d} - q)G + (u_{1d} - p) \sin \alpha}{\cos \alpha} \right]^2 = R^2 \quad (8)$$

Assuming that  $\begin{cases} A = R^2 \cos^2 \alpha - p^2 - G^2 q^2 - 2Gq \sin \alpha \\ B = -G^2 \\ C = -2G \sin \alpha \\ D = 2p + 2Gq \sin \alpha \\ E = 2G^2 q^2 + 2Gp \sin \alpha \end{cases}$  and  $\begin{cases} \alpha = \arcsin(-C/\sqrt{-4B}) \\ q = (-2E - DC)/(C^2 + 4B) \\ p = (2BD - EC)/(C^2 + 4B) \\ G = \sqrt{B} \\ R = \left[ \frac{4B(A + p^2 - Bq^2 - Cpq)}{C^2 + 4B} \right]^{\frac{1}{2}} \end{cases}$

Equation (8) can be written as follows:

$$u_{1d}^2 = A + Bu_{2d}^2 + Cu_{1d}u_{2d} + Du_{1d} + Eu_{2d} \quad (9)$$

Let  $y = u_{1d}^2; x_1 = u_{2d}^2; x_2 = u_{1d}u_{2d}; x_3 = u_{1d}; x_4 = u_{2d}$  and  $a_0 = A; a_1 = B; a_2 = C; a_3 = D; a_4 = E$  then Eq. (8) can be expressed as follows:

$$y = a_0 + a_1 x_1 + a_2 x_2 + a_3 x_3 + a_4 x_4 \quad (10)$$

Equation (10) is expressed in multivariable linear form. The coefficient determined by conducting linear regression based on the least squares principle possibly conforms to the matrix Eq. (11):

$$Qa = b \quad (11)$$

where,  $C = \begin{bmatrix} 1 & 1 & 1 & 1 & 1 \\ x_{10} & x_{11} & x_{12} & x_{13} & x_{14} \\ x_{20} & x_{21} & x_{22} & x_{23} & x_{24} \\ x_{30} & x_{31} & x_{32} & x_{33} & x_{34} \\ x_{40} & x_{41} & x_{42} & x_{43} & x_{44} \end{bmatrix}$ ,  $Q = (CC^T)$ , . and  $b = [y_0 \ y_1 \ y_2 \ y_3 \ y_4]^T$ .

By substituting  $x_i$  and  $y_i$  attained by performing two-path interference signal sampling into

the matrix Eq. (11), the correction parameters  $\alpha$ ,  $G$ ,  $p$ ,  $q$ , and  $R$  of interference signals can be obtained. Among the 5 parameters, the value of  $\alpha$ ,  $G$ ,  $p$ ,  $q$  will make error, but  $R$  parameter which is related to the amplitude of interference signal will not make error. By substituting these parameters into Eq. (12), the phase error induced by the three errors of the interference signals can be eliminated:

$$\begin{cases} u_1 = u_{1d} - p \\ u_2 = \frac{(u_{1d}-p) \sin \alpha + G(u_{2d}-q)}{\cos \alpha} \end{cases} \quad (12)$$

The three-error correction method is important to interference signal processing, in order to describe the method concisely. The two interference signals can also be represented by a vector. Let  $y_1 = u_{1d}$ ,  $x_1 = u_{2d}$ ,  $y_2 = u_1$ ,  $x_2 = u_2$ , then a vector  $\vec{r}_1 = x_1 i + y_1 j$  can be used to represent the two interference signals with three errors. As shown in Fig. 6(a), the elliptic curve (Lissajous curve) as shown in Eq. (8) can be obtained by vector  $\vec{r}_1$  rotation with the point  $o_1$ . and the parameters meaning related with three errors are also marked in the subgraph titled with “The signal before three errors correction”.  $\vec{r}_2 = x_2 i + y_2 j$  represents the two interference signals with three errors correction, a circular curve is obtained by vector  $\vec{r}_2$  rotation with the point  $o_2$ . The three errors detection module of the digital signal processing system realizes the detection of the parameters needed for three errors correction, and the phase calculation module realizes the calculation of the phase after three errors correction. The three errors of interference signals will lead to non-linear error during phase calculation. Generally, the non-linear error decreases from dozens of nanometers to nanometers [15]. For the system, the non-linear error decreases from about 20 nm to less than 2 nm, the result can be obtained from the data as shown in Fig. 6(b).

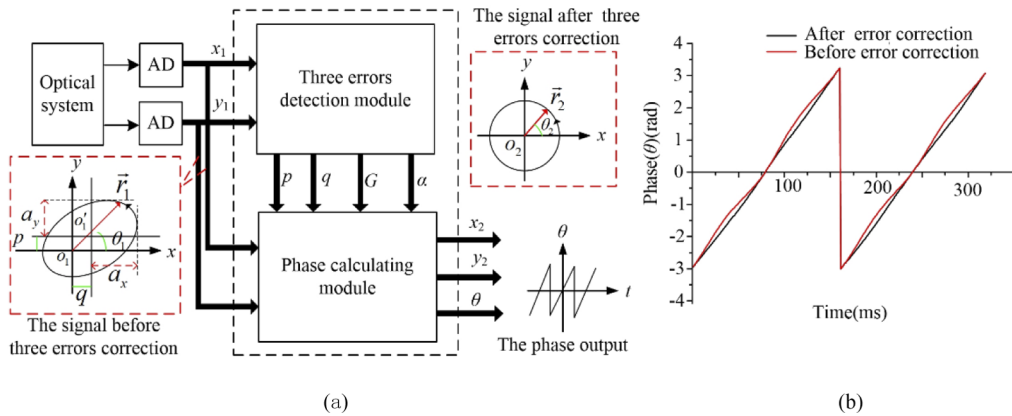


**Fig. 6.** The analytical model for error correction and phase calculation: (a) The components of the model; (b) One result with three-error correction.

### 3.3.2. Subdivision and counting of interference signals

After performing signal processing (involving filtering and three-error correction of interference signals), the phase calculation is applied to get the number of interference fringes. The interference fringes are subdivided and counted by hardware or software method. The methods of subdivision and counting for interference signal based on software and hardware are slightly different in terms of their modus operandi while having the same essential working principle. The interference fringes are counted based on combination of major number and minor number [16,17]. The difference is that the subdivision and counting based on software exhibits low real-time performance while that based on hardware presents high real-time performance; due to some technical measures such as post-processing, the subdivision and counting based on

software affords high flexibility during data processing. Thus, it generally has higher accuracy and reliability compared with subdivision and counting based on hardware. In terms of the basic technical route of subdivision and counting based on hardware, the interference signals are first shaped and judged in the moving direction and then the major number of interference fringes is counted by reversible counter while their minor number is obtained by the methods of computing or phase-locked frequency multiplication. Generally, subdivision and counting based on hardware presents inconsistency in counting position of major number and minor number of interference fringes, so it is necessary to link major and minor numbers of interference fringes. To avoid the occurrence of the linking of these numbers, the method of calculating all minor numbers first to attain the integral is proposed. In this way, seamless linking between major and minor numbers can be realized and the position at which the minor number periodically and abruptly changes corresponds to that at which the major number is counted. Through test validation, the method of subdivision and counting based on software overcomes the limitations of the method based on hardware and is applicable in the system.

### 3.4. Calculation of the refractive index and its error compensation

#### 3.4.1. Calculation of the refractive index

The number of interference fringes is subdivided and counted by using the signal processing software to attain the major number  $N$  and minor number  $\varepsilon$ . The optical path change induced by the refractive index of air is expressed as  $\Delta l = \frac{\lambda_0}{2} \cdot N + \varepsilon$  and thus the refractive index of air is calculated as  $n_{air} = 1 + \frac{\Delta l}{l}$ ;  $l$  refers to the cavity length (with a nominal length of 1000 mm) of the glass tube in the system, which can be measured by multiple methods. The length measurement of micro-cavity and high-precision cavity is generally conducted using an optical measurement method [18–21]. For the length measurement with ordinary accuracy, a length-measuring machine or coordinate measuring machine may be applied. The measurement accuracy of the cavity length is analyzed for the system. In the case that the measurement uncertainty is  $u(l) = 2\mu\text{m}$ ,  $k = 2$ , the uncertainty of the measurement of the refractive index of air is lower than  $3 \times 10^{-10}$ . Therefore, it is feasible that the cavity length of the glass tube is measured ( $L$  in mm) by applying a coordinate measuring machine with the uncertainty of  $(0.6 + L/800) \mu\text{m}$ .

#### 3.4.2. Source analysis and compensation for errors

If there are no error sources, the change  $\Delta l$  of the coherent length obtained from interference signals is that corresponding to the value of the refractive index of air; however, some error factors such as processing, installation, and adjustment errors of optical devices, difference of material temperature and deformation of the end-windows caused by vacuumization are inevitable. If error compensation is not performed, the measurement accuracy will be limited. The mechanism of action of various error factors is analyzed. Several error factors are analyzed, as follows:

##### 1. The quality and installation of optical devices

The geometrical quality (such as flatness of reflectors, parallelism of the end-windows, and geometric error of the KOSTER prism) of optical devices will influence the quality of interference fringes and generate the optical path error. To reduce these errors, on the one hand, an optical device needs to be measured and selected before being installed and used to ensure its geometric accuracy; on the other hand, optimizing the interference signals can compensate for the poor quality of signals induced by the processing quality of optical devices to some extent. The measurement system for the refractive index of air is based on the principle of measuring the double-beam optical path difference by vacuumization. This indicates that the measurement error of the refractive index of air does not occur if the geometric shapes of various parts of the optical system remain relatively unchanged

during measurement or only suffer common mode variation without causing an optical path difference through vacuumization.

To reduce the error caused by the installation and adjustment, the parallelism of two end faces of the vacuum tube is lower than 0.01 mm. The glass end-plate is optically cemented to the two end-faces of the vacuum tube, without light spots or shadows thereon. The vacuum tube is fitted with a Bessel supporting structure without constraint stress being induced.

## 2. Environmental factors

The influence of environmental factors on the system can be analyzed according to the components and working principle of the system (Fig. 1). The two laser beams (*i.e.*, measuring light M and reference light R) for double-beam interferometry are designed with equal optical path lengths. The performance of the equal optical paths can be examined by inputting a white light source into the system. Through tests, it can be found that the interference fringes of white light are significant, implying that optical paths are equal. In terms of the influence of environmental factors, the change of optical paths caused by temperature change at spatial positions of two light beams is considered. For example, due to the thermal deformation of materials, the non-uniform difference of temperature of devices along paths of the two light beams will lead to the optical path difference independent of the refractive index of air, thus resulting in measurement error. The two-path light beams are designed to be as close as possible to decrease the influence of the difference of environmental factors. Moreover, the protective cover from air disturbance is added. In addition, the influence of the change of material temperature on the refractive index of air is experimentally validated. Through tests and analysis, the environmental difference between the two optical paths in the system can be ignored. Among environmental parameters, air pressure mainly influences the change of the refractive index of air. The test result is shown in the form of curves in the top left of Fig. 7. The change in the refractive index of air is consistent with that of air pressure. Theoretically, the air temperature inversely influences the refractive index, that is, the refractive index decreases with increasing temperature, contrary to the influence of air pressure. The influence of temperature can be evaluated according to the fact that the rapid change of air pressure in the vacuum tube results in the sudden reduction of the temperature of the glass tube during rapid vacuumization. As shown in the locally amplified curve in the bottom right diagram in Fig. 7, the refractive index increases by about  $2 \times 10^{-7}$  when the temperature decreases by 0.04 °C. Although the change of material temperature will directly lead to the change of the length of the glass tube, the influence of the slight variation of the global length of the glass tube on the refractive index can be ignored due to the differential compensation effect of double-beam interference.

## 3. Pressure difference by vacuumization

The glass cavity with air through which the reference light travels needs to be vacuumized and maintained at a hard vacuum. During vacuumization, the glass cavity is compressed along the directions of axis and diameter. The end-window plates cemented to the glass cavity will experience slight deviation of the posture and thickness variation at the vacuumized area. The changes of the cavity length and diameter do not influence the optical path difference for measuring the refractive index of air while the deviation of the end-window plates and the change of thickness at the vacuumized area will affect the optical path difference. The change of thickness of end-window plates due to vacuumization was studied in detail elsewhere [14], and it is concluded that the thickness varies by 8 nm which is measured using F-P interferometry. End-windows, each with a thickness, of 6 mm are

used in the system. The displacement caused by the deformation of end-windows of the glass tube at the vacuumized area is measured by the interferometer using plane mirrors (Fig. 8). Through experiments, the displacement induced by the deformation of the end-windows during vacuumization in the system is 12 nm (Fig. 9). The measurement software directly compensates the error due to the pressure difference during vacuumization.

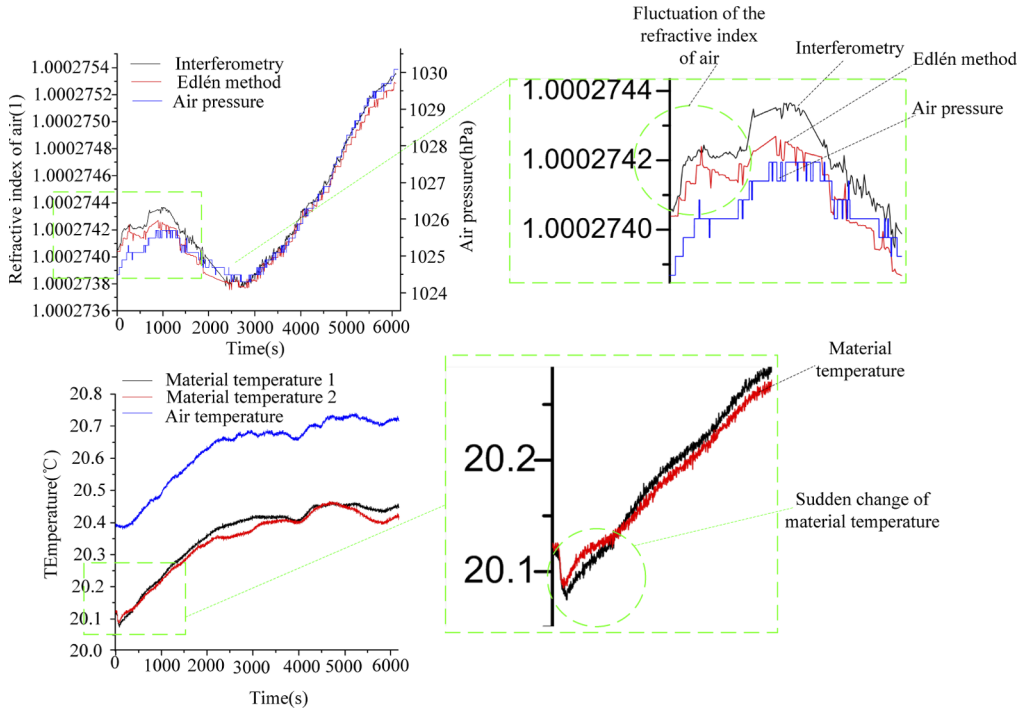


**Fig. 7.** Experimental result of influence of environmental changes on measurement of the refractive index of air.

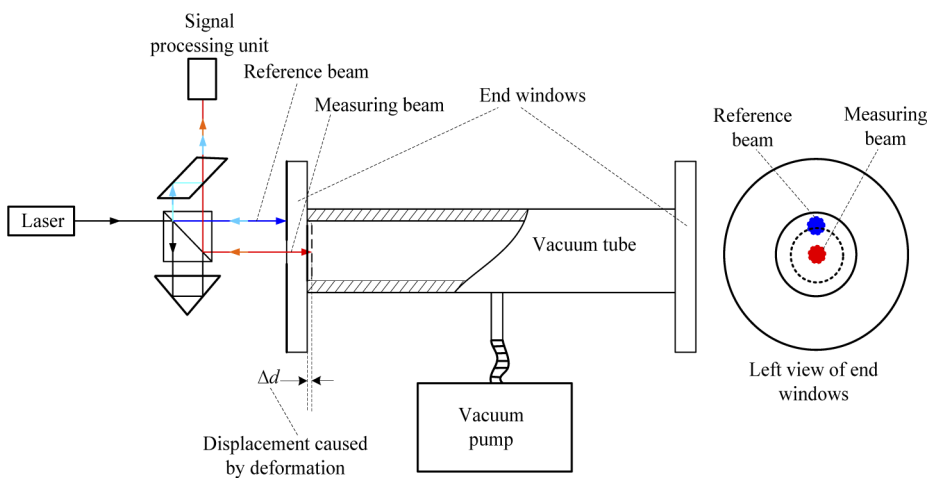


**Fig. 8.** Measurement principle of the displacement caused by the deformation of the end-windows of the vacuum tube.

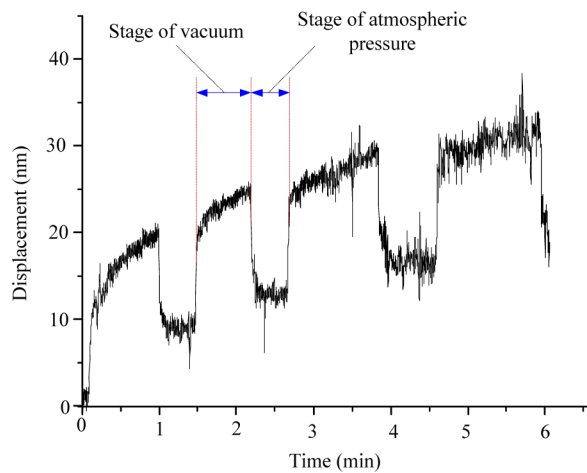


**Fig. 9.** The displacement caused by the deformation of each end-window of vacuum tube at the vacuumized position.

#### 4. Measurement experiment and result analysis

##### 4.1. Measurement experiment

The measurement of the refractive index of air was conducted on the system by comparing it with the formulaic method. The formula used is the latest Edlén empirical formula [22–25]. The method calculates the refractive index of air from the environmental parameters through Eqs. (13) to (16). The conversion relationships between physical parameters calculated through the equations are expressed in Fig. 10.

$$(n - 1)_s \times 10^8 = 8091.37 + \frac{2333983}{130 - \sigma^2} + \frac{15518}{38.9 - \sigma^2} \quad (13)$$

$$(n - 1)_x = (n - 1)_s[1 + 0.5327 \cdot (x - 0.0004)] \quad (14)$$

$$(n - 1)_{tp} = \frac{p(n - 1)_x}{93214.60} \cdot \frac{1 + 10^{-8}(0.5953 - 0.009876t)p}{1 + 0.0036610t} \quad (15)$$

$$n_{tpf} - n_{tp} = -f(3.8020 - 0.0384) \times 10^{-10} \quad (16)$$

where,  $(n-1)_s$  refers to the difference between the refractive index of air and the vacuum refractive index in standard conditions;  $(n-1)_x$  denotes the refractive index of air in which the content of CO<sub>2</sub> deviates by 400 ppm;  $(n-1)_{tp}$  denotes the relative refractive index of standard dry air at temperature  $t$  under pressure  $p$ ;  $(n_{tpf}-n_{tp})$  represents the difference of refractive index between moist air with partial pressure  $f$  of water vapour and dry air with the same total pressure;  $\sigma$ ,  $p$ ,  $t$ ,  $f$ , and  $x$  refer to the vacuum wave number ( $\mu\text{m}^{-1}$ ,  $\sigma = 1/\lambda$ ), air pressure (Pa), ambient temperature (°C), partial pressure of water vapour (Pa), and CO<sub>2</sub> content (mol) in air, respectively.

The accuracy of the latest Edlén empirical formula is  $U=1\times10^{-8}$  with  $k=2$ . For the temperature of the laboratory is controlled at standard 20 °C, the refractive index of air mainly varies with the change of the outside atmospheric pressure. To show the natural change in refractive index, we performed long-term measurements on different days using the same system. Figures 11 to 13 show the test results over separate three days: the absolute difference of values obtained by double-beam interferometry and the Edlén formula is less than  $4\times10^{-8}$ .

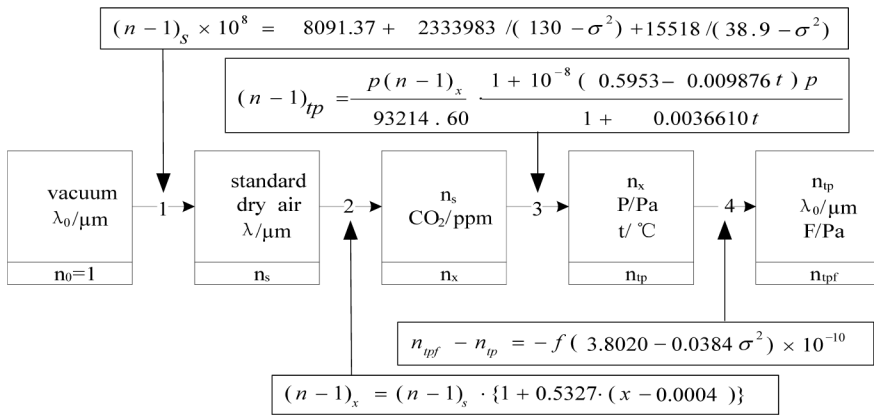


**Fig. 10.** Description of the physical meaning of the latest Edlén empirical formula.

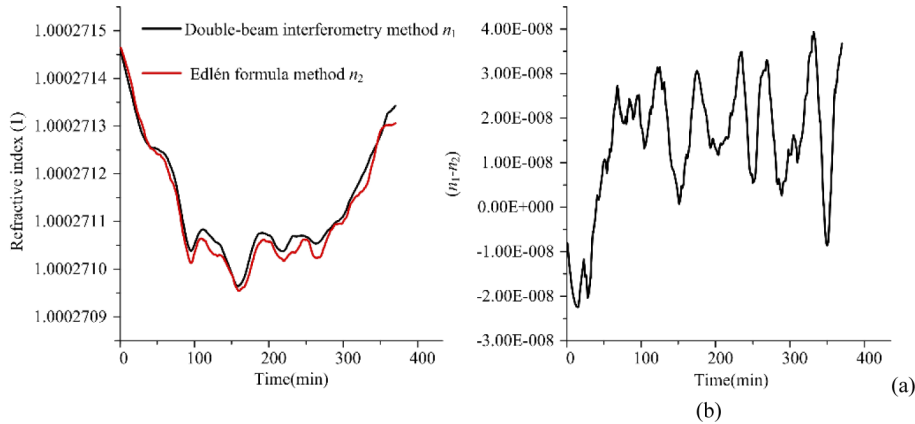


**Fig. 11.** Test results on 15 November 2019. (a) Measurement results of two methods. (b) The result differences between two methods.

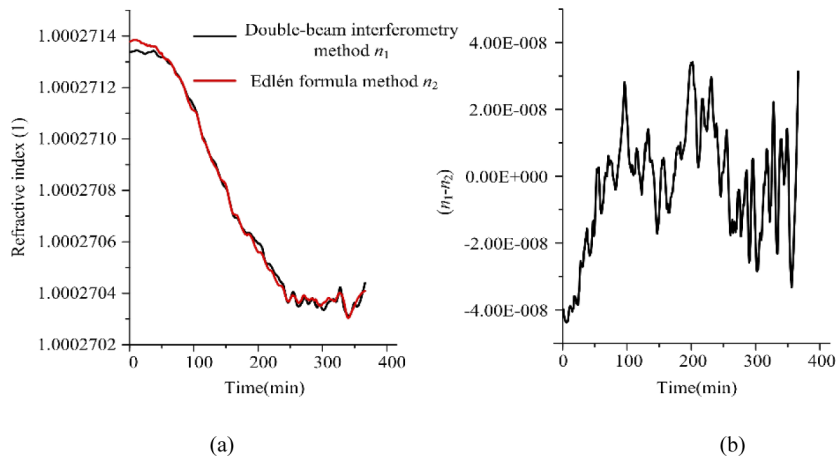


**Fig. 12.** Test results on 21 November 2019. (a) Measurement results of two methods. (b) The result differences between two methods.

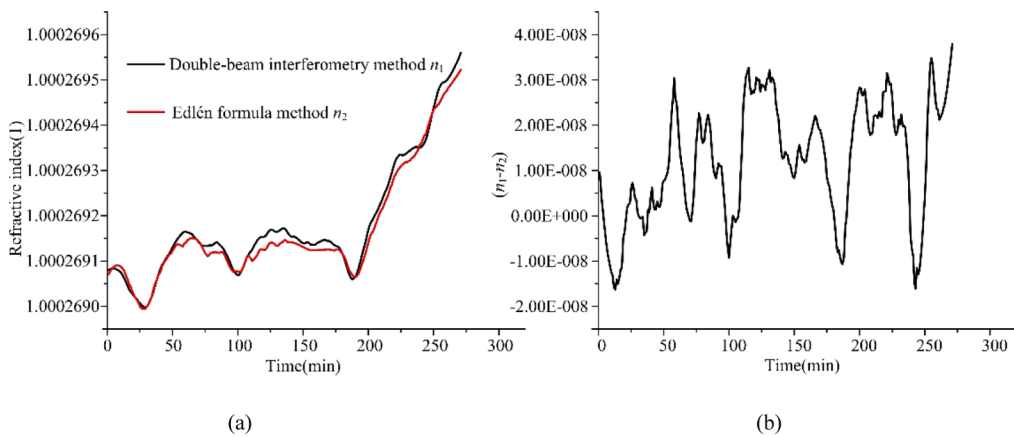


**Fig. 13.** Test results on 15 November 2019. (a)Measurement results of two methods. (b)The result differences between two methods.

#### 4.2. Analysis

The Edlén formula method is improved in accuracy after several upgrades [22–24]; however, the formula itself has an error of at least  $1 \times 10^{-8}$  owing to its being formed on the basis of experience and relatively lower accuracy than that achieved using interferometry. The Edlén formula method does show its advantages, including easy installation of hardware of the system, and high reliability. In contrast, although the interferometry presents high accuracy, it shows a relatively complex system. Moreover, there are more factors influencing the measurement result, thus relatively onerous technical requirements were imposed. Therefore, the basic thinking is to analyze the measurement uncertainty of the air refractive index measured by double-beam interferometry, and then verify the  $E_n$  value of the measurement result obtained by the Edlén formula method.

Equation (2) shows the theoretical mathematical model for measuring the refractive index of air, which can be further expressed as follows:

$$n_{air} = \frac{\Delta l}{l} + 1 = \frac{\lambda_0 N}{2l} + 1 \quad (17)$$

where,  $\lambda_0$ ,  $N$ , and  $l$  refer to the laser wavelength, the number of interference fringes on the optical path induced by the refractive index of air, and the sampling length (that is, the cavity length of the glass tube) for measurement, respectively. In view of various error correction factors, the mathematical model for measurement error of the refractive index of air can be expressed by Eq. (18):

$$\delta n = \frac{N}{2l} \delta \lambda_0 + \frac{\lambda_0}{2l} \delta N - \frac{\lambda_0 N}{2l^2} \delta l + \delta n_{xb} + \delta n_{py} + \delta n_{zkd} + \delta n_{wd} + \delta n_{prl} \quad (18)$$

where,  $\delta \lambda_0$ ,  $\delta N$ ,  $\delta l$ , and  $\delta n_{xb}$  represent the error of laser wavelength, the error of the count of interference fringes, the error of the length of the glass cavity, and the error induced by the displacement of sealed end-windows of the glass cavity at the vacuumized area, respectively;  $\delta n_{zkd}$ ,  $\delta n_{wd}$ , and  $\delta n_{prl}$  denote the errors incurred by the degree of the vacuum, non-uniform transverse temperature distribution, and the change of the angle between the two end-window planes of the glass cavity, respectively.

Evaluation of measurement uncertainty is an indispensable part of any measurement system. The analysis and evaluation were carried out according to international standard JGCM 100: 2008 [25], Table 1 lists various error sources and their sensitivity coefficients in the error propagation equation as well as various uncertain measurement components. According to Table 1, the

combined standard uncertainty is expressed as  $u_c = 2.5 \times 10^{-9}$ . By setting the coverage factor  $k$  to 2, the expanded uncertainty  $U$  is  $5.0 \times 10^{-9}$ . The best result of the traditional method which is based on same optical principle is about  $2.0 \times 10^{-8}$ , so the accuracy of the system is about four times more accurate than traditional one.

**Table 1. Evaluation of measurement uncertainty.**

$x_i$	Symbol	$c_i = \delta l / \delta x_i$	$u(x_i)$	$u_i (l)$
$\lambda_0$	$u_1$	$4.3 \times 10^{-3} \mu\text{m}^{-1}$	$1.0 \times 10^{-8} \lambda_0$	$3.0 \times 10^{-12}$
$N$	$u_2$	$3.2 \times 10^{-7}$	0.006	$1.9 \times 10^{-9}$
$l$	$u_3$	$2.7 \times 10^{-10} \mu\text{m}^{-1}$	1 $\mu\text{m}$	$2.7 \times 10^{-10}$
$n_{xb}$	$u_4$	1	$1.0 \times 10^{-9}$	$1.0 \times 10^{-9}$
$n_{zkd}$	$u_5$	1	$0.4 \times 10^{-10}$	$0.4 \times 10^{-10}$
$n_{wd}$	$u_6$	1	$0.1 \times 10^{-10}$	$0.1 \times 10^{-10}$
$n_{prl}$	$u_7$	1	$1.3 \times 10^{-9}$	$1.3 \times 10^{-9}$

Through test data, it shows that the absolute value of the difference between the result  $R_1$  obtained based on double-beam interferometry and  $R_2$  obtained based on the Edlén empirical formula conforms to  $|R_1 - R_2| < 4.0 \times 10^{-8}$ , in which the uncertainty of  $R_1$  is  $U_1 = 5 \times 10^{-9}$ , with  $k = 2$  while that of  $R_2$  is  $U_2 = 6 \times 10^{-8}$ , with  $k = 2$ . They are verified through the  $En$  value:

$$En = \frac{|R_1 - R_2|}{\sqrt{U_1^2 + U_2^2}} \quad (19)$$

Through calculation based on Eq. (19), it is found that  $En < 1$ , indicating that the uncertainty of the measurement results is reasonable.

## 5. Conclusion

The accuracy of laser wavelength measurement in air is the main factor restricting the accuracy of the length measurement primary standard. Realizing the high-accuracy measurement of the refractive index of air to attain accurate laser wavelength in air environment has been the research focus of length metrology researchers for many years. By taking the traditional double-beam interferometry as the basic principle, a simple high-accuracy measurement system for the refractive index of air is realized. The system shows technical innovations in different technical aspects concern with interference optics, signal sampling and recording, signal processing. The optical system is simple, and the signal processing system is adaptable. The error compensation is investigated to improve the measurement accuracy of the system. A comparison is made between measurement results obtained separately through the system and the Edlén empirical formula. Through tests and analysis of measurement results, it can be concluded that the measurement uncertainty can satisfy the high-accuracy measurement requirement of the length measurement primary standard for the compensation of refractive index of air in the uncertainty  $U = 5 \times 10^{-9}$ , with  $k = 2$ . The system may be optimized further to be applied popularly in a few technical aspects. The length of the vacuum glass tube may be shortened through optical multiplication to reduce overall system volume, technical means should be studied to avoid to be pertaining to utilization of the vacuum pump after one of vacuumization.

**Funding.** National Key Research and Development Program of China (2017YFF0204803); Capacity Improvement Program of the State Administration for Market Regulation of China (24-ANL1804); Special Scientific Research on Civil Aircraft of Ministry of Industry and Information Technology of the People's Republic of China (MJ-2018-J-70).

**Disclosures.** The authors declare that there are no conflicts of interest related to this article.

## References

1. P. Hariharan, "Basics of Interferometry," Elsevier Inc, Sydney, Australia (1992).
2. P. F. Egan and J. A. Stone, "Absolute refractometry of dry gas to  $\pm 3$  parts in 109," *Appl. Opt.* **50**(19), 3076–3086 (2011).
3. E. J. Jung, W. J. Lee, M. J. Kim, S. H. Kwang, and B. S. Rho, "Air cavity-based Fabry–Perot interferometer sensor fabricated using a sawing technique for refractive index measurement," *Opt. Eng.* **53**(1), 017104 (2014).
4. P. F. Egan, J. A. Stone, J. H. Hendricks, J. E. Ricker, G. E. Scace, and G. F. Strouse, "Performance of a dual Fabry–Perot cavity refractometer," *Opt. Lett.* **40**(17), 3945–3948 (2015).
5. J. Zhang, Z. H. Lu, and L. J. Wang, "Precision measurement of the refractive index of air with frequency combs," *Opt. Lett.* **30**(24), 3314–3316 (2005).
6. K. Minoshima, K. Arai, and H. Inaba, "High-accuracy self-correction of refractive index of air using two-color interferometry of optical frequency combs," *Opt. Express* **19**(27), 26095–26105 (2011).
7. G. Wu, K. Arai, M. Takahashi, H. Inaba, and K. Minoshima, "High-accuracy correction of air refractive index by using two-color heterodyne interferometry of optical frequency combs," *Meas. Sci. Technol.* **24**(1), 015203 (2013).
8. Q. Chen, H. Luo, S. Wang, F. Wang, and X. Chen, "Measurement of air refractive index fluctuation based on interferometry with two different reference cavity lengths," *Appl. Opt.* **51**(25), 6106–6110 (2012).
9. T. Pikálek and B. Zdeněk, "Air refractive index measurement using low-coherence interferometry," *Appl. Opt.* **54**(16), 5024–5030 (2015)..
10. P. Huang, J. Zhang, Y. Li, and H. Wei, "Note: Real-time absolute air refractometer," *Rev. Sci. Instrum.* **85**(5), 056107 (2014)..
11. K. Minoshima, K. Arai, and H. Inaba, "High-accuracy self-correction of refractive index of air using two-color interferometry of optical frequency combs," *Opt. Express* **19**(27), 26095–26105 (2011).
12. R. Schödel, F. Pollinger, A. Nicolaus, G. Bartl, T. Schulte, and N. Bhattacharya, "Modern Interferometry for Length Metrology Exploring limits and novel techniques," IOP Publishing, Bristol, UK (2018).
13. G. Bönsch and E. Potulski, "Measurement of the refractive index of air and comparison with modified Edlén's formulae," *Metrologia* **35**(2), 133–139 (1998).
14. P. Q. Liu and Y. K. Zhao, "The historical contribution of Bernoulli's equation to the establishment of fluid mechanics theory," *Mech. Eng.* **42**(2), 258–264 (2020).
15. C. M. Wu, C. S. Su, and G. S. Peng, "Correction of nonlinearity in one-frequency optical interferometry," *Meas. Sci. Technol.* **7**(4), 520–524 (1996).
16. Y. Z. Yang, B. Y. Chen, X. W. Wu, and D. C. Li, "A novel interference fringes software counting method," *Proc. SPIE* **5638**, 722–728 (2005).
17. Z. Y. Wang, H. T. Chang, H. T. Gao, and X. Y. Ye, "FPGA-based signal processing method of automatic interference comparator," *Proc. SPIE* **8916**, 89161X (2013).
18. R. Illingworth and I. S. Ruddock, "Cavity length measurement for synchronously pumped, mode-locked lasers," *Opt. Commun.* **59**(5–6), 375–378 (1986).
19. Q. Ji, X. R. Ma, J. Sun, H. Zhang, and Y. Yao, "Novel method for measurement of effective cavity length of DBR fiber," *Chin. Opt. Lett.* **8**(4), 398–400 (2010).
20. C.J. Curtis, J.C. Dahlberg, W.A. Oren, and K.J. Tremblay, "The measurement of the optical cavity length for the Infrared Free-Electron Laser," United States, <https://www.osti.gov/servlets/purl/754629>.
21. A. Staley, D. Hoak, A. Effler, K. Izumi, S. Dwyer, K. Kawabe, E. J. King, M. Rakhamanov, R. L. Savage, and D. Sigg, "High precision optical cavity length and width measurements using double modulation," *Opt. Express* **23**(15), 19417–19431 (2015)..
22. B. Edlén, "The dispersion of standard air," *J. Opt. Soc. Am.* **43**(5), 339–344 (1953).
23. B. Edlen, "The refractive index of air," *Metrologia* **2**(2), 71–80 (1966).
24. K. P. Birch and M. J. Downs, "An updated Edlén equation for the refractive index of air," *Metrologia* **30**(3), 155–162 (1993).
25. Joint Committee for Guides in Metrology., "Evaluation of Measurement data -Guide to the Expression of Uncertainty in Measurement," *JGCM* **100**, 2008.